Apparent Activation Energy of Coal Oxidation with Different Particle Sizes based on Temperature-programmed Approach

Zhao J.Y.[1,2,3,] *, Zhang Y.X.[1,2], Deng J.[1,2], Shu C.M.[4,] *, Cheng Y.C.[4], Yi X.[1,2]

[1] *Xi'an University of Science and Technology, Xi'an, China*
[2] *Shaanxi Key Laboratory of Prevention and Control of Coal Fire, Xi'an, China*
[3] *Institute for Arid Ecology and Environment, Urumqi, China*
[4] *National Yunlin University of Science and Technology, Yunlin, Taiwan, ROC*
**Corresponding author's email: zhaojingyu2014@126.com*

ABSTRACT

To study the effect of coal particle size on the activation energy of coal oxidation reaction in different oxidation stages, the experimental equipment of temperature-programmed tests was adopted. To determine the relationship between oxygen consumption rate and gas products, the temperature was explored in the low-temperature oxidation stage of coal samples with different particle sizes. The critical temperature point for coal samples of different particle sizes was obtained by analyzing the change rule of gas product and oxygen consumption rate with temperature, and dynamic analysis was carried out on this basis. Establishing an Arrhenius formula between the oxygen consumption rate and the coal temperature, the apparent activation energy equation was obtained from the logarithmic treatment method. The linear regression on straight line gradient of the equation was analyzed and the apparent activation energy for the low temperature oxidized coal sample was calculated. The results showed that the particle sizes affected the apparent activation energy, and the larger the particle size was, the larger the activation energy was. However, the coal samples with a particle size of 5–7 mm had the maximum apparent activation energy before the critical temperature. Compared with other particle sizes, the coal sample of this particle size did spontaneously combust easily.

KEYWORDS: Coal oxidation, oxygen consumption, critical temperature, dynamic analysis, spontaneous combustion.

NOMENCLATURE

A	Pre-exponential factor s^{-1}	Q	Air supply volumetric flow rate mL/s
A_{ad}	Ash content air-dried basis %	R	Universal gas constant 8.314 J mol^{-1} K^{-1}
E	Apparent activation energy kJ mol^{-1}	S	Test tube sectional area cm^2
FC_{ad}	Fixed carbon content air-dried basis %	T	Temperature °C
L	Height of coal sample cm	V_{ad}	Volatile matter content air-dried basis %
M_{ad}	Moisture content air-dried basis %	V_m	Volume of the experimental coal sample cm^3
n	Reaction order dimensionless		

INTRODUCTION

As an economical and low-cost energy source, coal accounts for the largest share of global electricity production. However, spontaneous combustion of coal has been, and continues to be, a major threat associated with the extraction and storage of coal. Once this happens, it can cause

Proceedings of the Ninth International Seminar on Fire and Explosion Hazards (ISFEH9), pp. 1144-1153
Edited by Snegirev A., Liu N.A., Tamanini F., Bradley D., Molkov V., and Chaumeix N.
Published by Saint-Petersburg Polytechnic University Press
ISBN: 978-5-7422-6498-9 DOI: 10.18720/spbpu/2/k19-62

major problems, such as huge losses of coal resources, environmental damage, and death [1-3]. In underground coal mining, spontaneous combustion usually occurs in concealed areas, such as inaccessible gobs. Research on the characteristics of spontaneous combustion is useful for monitoring and assessing the severity of coal fires, as well as preventing and controlling them.

The low-temperature oxidation reaction is complex and varies with the temperature [4-6]. The spontaneous combustion tendency of coal reflects the easy degree of coal spontaneous combustion and the low-temperature oxidation characteristics [7, 8]. Coal oxidation is an irreversible exothermic process, and the reaction rate increases with increasing temperature [9-12]. To predict this critical temperature, numerous methods have been established, such as adiabatic oxidation, temperature programmed and exponential gas growth rates. In recent years, the influence of particle size on combustion reactions has received increasing attention. Some scholars have studied this effect in the study of coal spontaneous combustion. The effects of coal particle size on kinetic parameters (apparent activation energy, reaction rate), exothermic intensity and oxygen consumption rate in coal oxidation and pyrolysis have been studied [13-16].

At present, many scholars are carrying out kinetic analysis of coal samples with different degrees of metamorphism by using thermal analysis experiments, and testing the effects of various influencing factors such as oxygen concentration, particle size and heating rate on activation energy [17-23]. Gao conducted a simultaneous thermal analyzer (STA) experiment to explore the relationship between the apparent activation energy of coal and heating rate and oxygen concentration. The bituminous coal samples were analyzed using a simultaneous thermal analyzer [24]. Wang studied the mass gain of coal oxidation observed by thermogravimetric analysis. Thermogravimetric infrared and thermogravimetric in-situ infrared experiments were carried out on a typical Jurassic coal in western China, and the kinetics and mechanism of coal oxidation were determined [25, 26]. The scholars mentioned that the above used fewer coal samples, and the critical temperature was used as a key temperature point for coal in the low-temperature oxidation stage; there were few macroscopic experiments near this temperature point. Therefore, it is meaningful to perform a segmentation calculation of the activation energy of the low-temperature oxidation process of coal with the critical temperature as the segmentation point.

In this paper, the critical temperature of coal spontaneous combustion was measured by the temperature-programmed experimental system. The gas products of different particle sizes were obtained, and the apparent activation energy was calculated. The relationship between particle size and coal spontaneous combustion tendency was obtained, and the spontaneous combustion tendency of coal in different coal seams was studied.

EXPERIMENTAL

Coal sample preparation

The coal samples of the 2^{-2mid} and 3^{-1} coal seams in Wantugou coal mine were selected as long-flame coal samples. The samples were divided into two groups. Each group was pulverized in the air, and the coal was screened according to the five particle sizes of 0–0.9, 0.9–3, 3–5, 5–7, 7–10 mm. Each of the five particle sizes was screened at 1.2 kg, and each particle size was used to complete the experiment with 1.0 kg; the remaining 200 g was composed of the mixed coal sample. Coal quality was established by proximate and ultimate analyses, the results (Table 1) are presented on an air-dried basis.

Experimental apparatus

A self-designed temperature-programmed experimental system was employed to investigate the characteristics of coal spontaneous combustion during the decaying process. The experimental

system consisted of three parts: gas supply system, temperature-programmed system, and gas sample analysis system. The gas supply system can provide a variety of oxygen content of the carrier gas for the oxidation of coal. The temperature-programmed system consists of an oven, a sample reactor and a thermocouple sensor inserted into the center of the reactor. The inner surface of the oven is insulated with asbestos and stainless material. The sample reactor is a cylindrical body with a diameter of 9.5 cm and a length of 25 cm. Before entering the sample reactor, the carrier is preheated by a long curved copper tube. Gas sample analysis systems include gas chromatograph and computer. Figures 1 (a) and (b) show the schematic of the reactor.

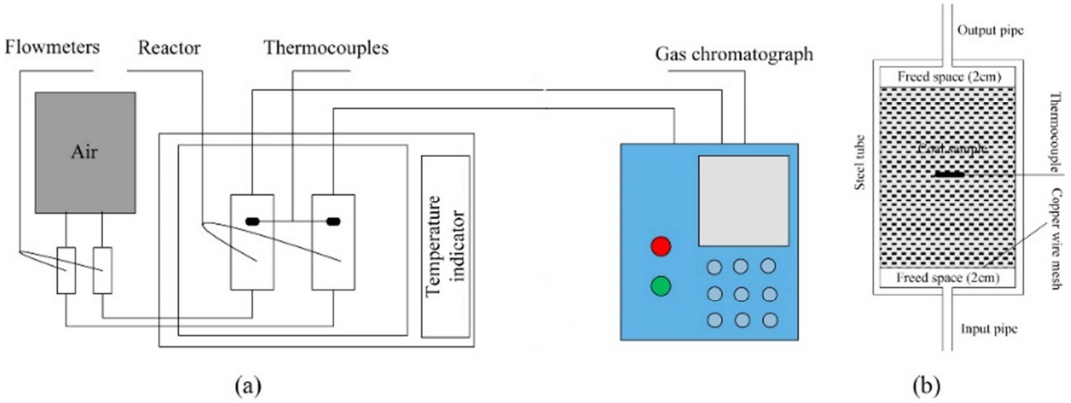

Fig. 1. Temperature-programmed experimental system: (a) overall picture and (b) reactor enlargement.

At the beginning of the experiment, the coal sample was first put into the reactor, and then into the heating box to connect the gas path which was open to the air pump, the flow rate to 120 mL/min, ventilation started to pick up an hour later, the heating rate 0.3 °C/min. Since 30 °C, using gas chromatograph analysis of gas composition, every 10 °C temperature interval of half an hour to receive gas analysis, the end of the experiment temperature was 170 °C. A total of 15.0 gas extraction analyses were conducted. Then the heating was stopped. Finally, the gas source was closed, and the experiment was finished.

Table 1. Analysis of coal quality of experimental coal samples

Sample	M_{ad} (%)	A_{ad} (%)	V_{ad} (%)	FC_{ad} (%)
2^{-2mid}	6.44	6.45	29.60	57.51
3^{-1}	8.73	7.23	47.43	42.61

RESULTS AND DISCUSSION

CO gas analysis

CO gas was selected as the index gas for different stages of the low-temperature oxidation process of coal. It can be seen from Fig. 2(a) that the CO emission of coal samples with different particle sizes in the 2^{-2mid} coal seam at normal temperature was almost the same. With the increase in temperature, the release amount of CO gas had a large change, and the gas release amount was measured at 170 °C. The gap was exceptionally obvious, and the law was that as the particle size increased, the amount of CO gas released decreased, while the amount of CO gas released from the sample was moderate. The CO gas generated by different particle sizes on coal samples showed two mutations during the heating process. The first abrupt temperature changed with the particle size, 0–0.9 mm particle size, 0.9–3 mm particle size. The temperature point of the mixed sample was 60 °C,

the temperature point of the particle diameter of 3–5 mm was 70 °C, and the temperature point of the particle diameter of 5 to 7 mm and 7–10 mm was 80 °C, which indicated that the larger the particle size, the first abrupt temperature. The later the hysteresis, the temperature of the abrupt was the critical temperature of the coal sample. After the critical temperature, the growth rate of CO gas was significantly higher than the critical temperature, and the second abrupt temperature occurred. 120 °C, which indicated that the temperature was the dry cracking temperature of the coal sample; the gas growth rate was close to exponential growth after this temperature point.

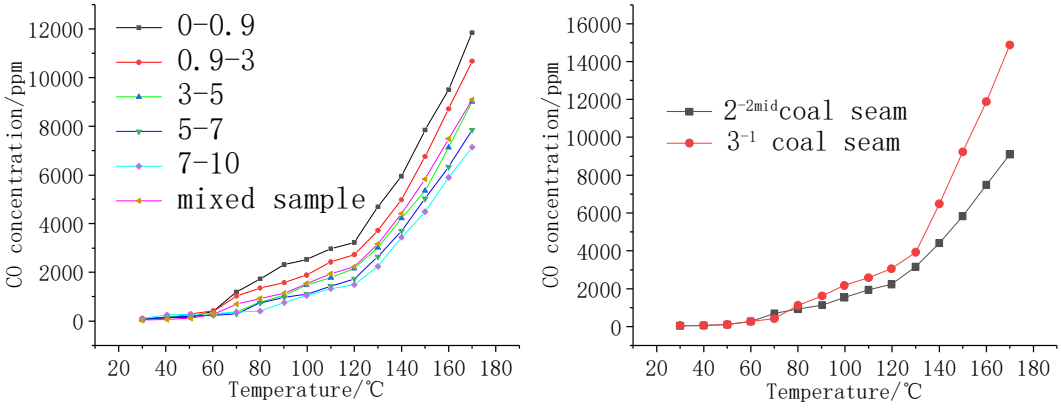

(a) (b)

Fig. 2. CO gas and temperature curve of coal sample: (a) different particle sizes and (b) different coal seams.

C_2H_4 gas analysis

C_2H_4 gas was selected as the index gas to assist in the different stages of low-temperature oxidation of coal. It can be seen from Fig. 3(a) that the C_2H_4 gas produced by the coal samples with different particle sizes of the same coal seam increased with the increase of temperature. At the same temperature point, as the particle size increased, the amount of gas released was less, and the mixture was mixed. The amount of gas released was at a moderate level. The gas appears at a temperature point of 80 to 100 °C; the law is that the temperature point lags with the increase of the particle size, while the mixed sample is in the centered position. Moreover, the growth rate of the gas before the cracking temperature was relatively slow; the cracking temperature shows an exponential growth.

It can be seen from Fig. 3(b) that under the condition that the particle size is the same as the mixed sample, the amount of C_2H_4 gas released by the 3^{-1} coal sample was larger than that of the coal sample of 2^{-2mid}, and the temperature at which the gas was generated was also earlier than that of the coal in 2^{-2mid}. Similarly, the temperature point at which the gas amount was abrupt was also delayed by 10 °C in the 2^{-2mid} coal sample.

Analysis of the oxygen consumption rate

The gas source used in this experiment was air, so the oxygen concentration at the inlet of the coal sample tank was 21 vol.%, and the oxygen concentration at the outlet could be measured by gas chromatography, so that the oxygen consumption rate of the coal sample can be calculated and the temperature was obtained by law of change.

The oxygen consumption rate of the coal sample in the sample reactor is expressed by Eq. (1):

$$v_{o_2}^0 = \frac{QC_{O_2}^0}{SL} \cdot ln\frac{C_{O_2}^1}{C_{O_2}^2} = \frac{QC_{O_2}^0}{V_m} \cdot ln\frac{C_{O_2}^0}{C_{O_2}^2} \quad (1)$$

where $v_{o_2}^0(T)$ is the average rate of oxygen consumption per unit volume of coal sample in fresh air current, mol/(cm^3·s) ; $C_{O_2}^0$ is the oxygen concentration in fresh airflow, $C_{O_2}^0$ = 9.375×10^{-6} mol/mL; Q is the air supply volume, mL/s; S is the test tube sectional area, cm^2; L is the height of coal sample, cm; $C_{O_2}^1$, $C_{O_2}^2$ is the oxygen concentration at the inlet and outlet of the coal sample, $C_{O_2}^1$ = $C_{O_2}^2$ = 9.375×10^{-6} mol/mL; V_m indicates the volume of the experimental coal sample, cm^3.

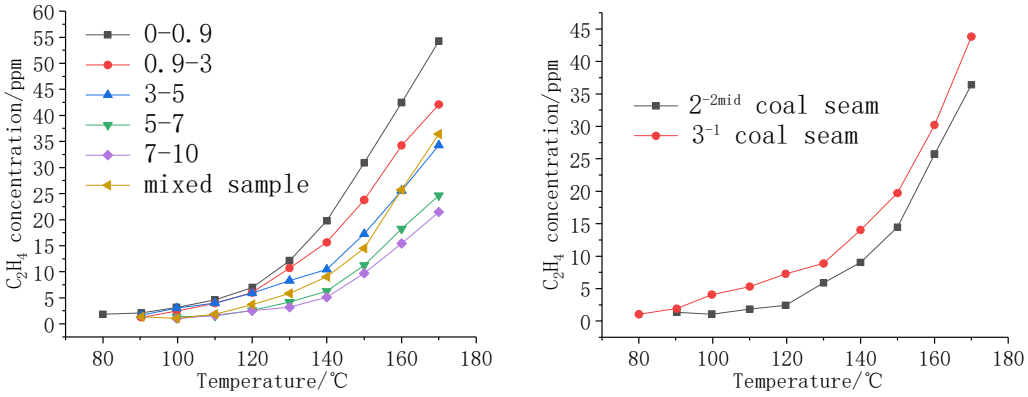

(a) (b)

Fig. 3. C_2H_4 gas and temperature curve of coal sample: (a) different particle sizes (b) different coal seams.

According to Eq. (1), curves of oxygen consumption rates with different particle sizes and coal types can be obtained.

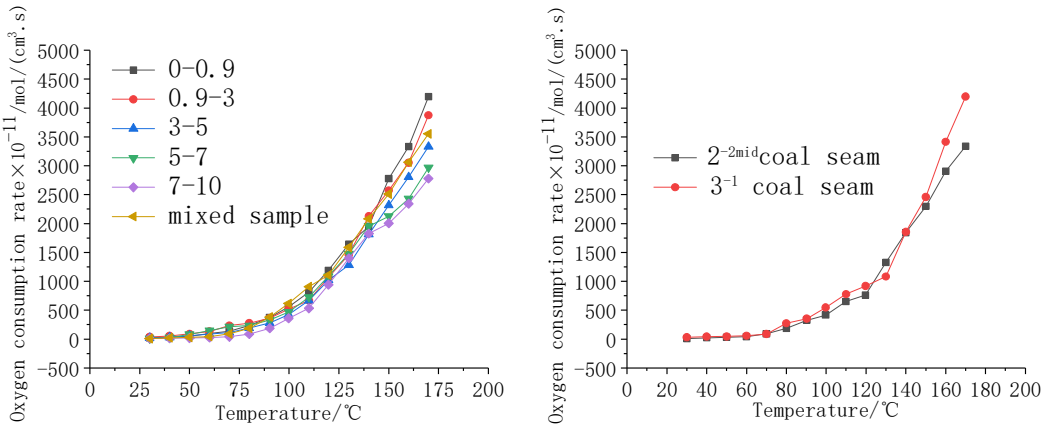

(a) (b)

Fig. 4. Oxygen consumption rate and temperature curve of coal sample: (a) different particle sizes and (b) different coal seams.

It can be seen from Fig. 4(a) that the oxygen consumption rate of coal samples with different particle sizes of the same coal seam increased with the increase of temperature. When at the same temperature point, the law showed that the oxygen consumption rate was lower as the particle size increased, and the oxygen consumption rate of the mixed sample was at a higher level. Before the critical temperature, the oxygen consumption rates of different particle sizes were not much different. At the critical temperature, the oxygen consumption rate demonstrated the first mutation,

and after the critical temperature, its growth rate increased significantly. At the cracking temperature, the second abrupt temperature occurred, and then the rate of oxygen consumption showed exponential growth.

It can be seen from Fig. 4(b) that when the particle size was mixed, the oxygen consumption rate of the 3^{-1} coal seam was substantially larger than that of the 2^{-2mid} coal seam, because the dry cracking temperature of the 3^{-1} coal seam was greater than the coal seam of 2^{-2mid}, so at 130 and 140 °C, the oxygen consumption rate of the 3^{-1} coal seam was less than 2^{-2mid} coal seam.

By analyzing the change law of CO and C_2H_4 gas and oxygen consumption rate with temperature, the critical temperature point was obtained, and the dynamic analysis was carried out by dividing the stage.

Oxidation kinetics analysis

During the spontaneous combustion of coal, the surface of the coal body is chemically adsorbed and oxidized by oxygen molecules, releasing many gases and a large amount of heat.

Coal + O_2 → mCO + gCO_2 + other products

According to the reaction rate calculation method and the Arrhenius equation, the reaction rate obeys the first-order Arrhenius equation, and Eq. (2) is obtained as follows:

$$v_{o_2}(T) = AC_{o_2}^n exp\left(-\frac{E_a}{RT_i}\right) \tag{2}$$

where $v_{o_2}(T)$ is the actual oxygen consumption rate, mol/(cm^3·s); A is the pre-exponential factor; E_a is the activation energy; and R is the gas constant, R=8.314 J/(mol·K), n is the reaction order, taking n = 1; C_{O_2} indicates the oxygen content in the reaction gas, mol/cm^3.

Combining Eqs. (1) and (2), the formula for calculating the oxygen consumption rate and activation energy can be determined:

$$v_{o_2}^0(T) = AC_{o_2}^0 exp\left(-\frac{E_a}{RT_i}\right) \tag{3}$$

Further, simplifying the formula in Eq. (3), that is, taking the logarithm on both sides:

$$\text{Ln}\, v_{o_2}^0 = \ln A + \ln C_{o_2}^0 - \frac{E_a}{RT_i} \tag{4}$$

Finishing up:

$$\ln \frac{v_{o_2}^0}{C_{o_2}^0} = -\frac{E_a}{RT_i} + \ln A \tag{5}$$

It can be seen from the formula that in the Cartesian coordinate system, $\ln(v_{o_2}^0/C_{o_2}^0)$ is the ordinate and $1/T$ is the abscissa, and the data can be fitted to a straight line. The slope of the line can be used to calculate the apparent activation energy. By taking the different particle sizes of the same coal seam and the oxygen consumption rate of different coal seam samples into the above formula, the apparent activation energy of the coal sample can be obtained. Since the apparent activation energy of coal samples before and after the critical temperature was quite different, the Arrhenius curves of different coal seams and different particle sizes before and after the critical temperature are, respectively, fitted, as shown in Figs. 5 and 6.

According to the above fitting curve, the activation energies corresponding to the critical temperatures of different coal samples are summarized as given in Table 2.

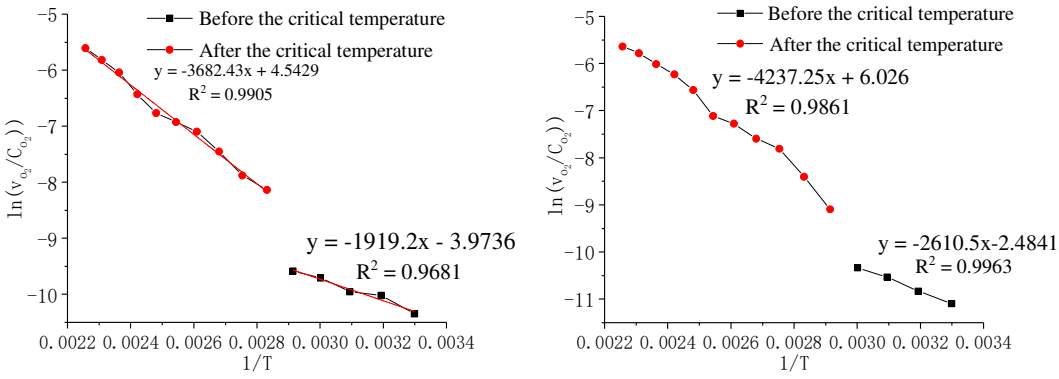

Fig. 5. $\ln(v_{o_2}^0/C_{o_2}^0)$ and 1/T relative curves of mixed coal seams: (a) 2-2mid coal sample mixed sample and (b) 3-1 coal sample mixed sample.

Table 2 Apparent activation energy of different coal samples

Coal sample number	Critical temperature, °C	E_1, kJ/mol	E_2, kJ/mol
0–0.9	60.0	17.06	29.57
0.9–3	60.0	23.25	37.46
3–5	70.0	27.40	41.28
5–7	80.0	34.97	41.75
7–10	80	33.44	44.63
2^{-2mid} mixed sample	60	21.70	35.22
3^{-1} mixed sample	70	15.95	30.61

It can be seen from Table 2 that with the increase of the particle size of the coal sample, the apparent activation energy before the critical temperature basically shows an increasing situation, which is because the smaller the particle size of the coal sample, the specific surface area of its reaction with oxygen. The larger, the more active coal molecules were exposed at the same time, so the easier it was to react with oxygen, which, in turn, generated more heat and accelerated the reaction. The apparent activation energy after the critical temperature also showed that the apparent activation energy increased as the particle size increased. That mentioned above was because, after the critical temperature, the macromolecular structure in the coal body accelerated the fracture, increasing the number of active groups. In addition, the larger the particle size, the smaller the specific surface area, and the less likely it was to react with oxygen. The apparent activation energy after the critical temperature was much larger than before the critical temperature, because the reaction before the critical temperature consumed a large amount of unstable reactive functional groups in the coal molecules, and the critical temperature requires a more stable functional group structure. Therefore, the reaction was more difficult than before. The apparent activation energy required for the mixed reaction was less because the mixed sample contained all the particle diameters, and its specific surface area was relatively large, and its reaction with oxygen was relatively easy to occur. At the same time, under the same coal quality conditions, the particle size of 5–7 mm in the early stage of the reaction showed a difference: it was the critical particle size. Accordingly, the apparent activation energy required was the largest.

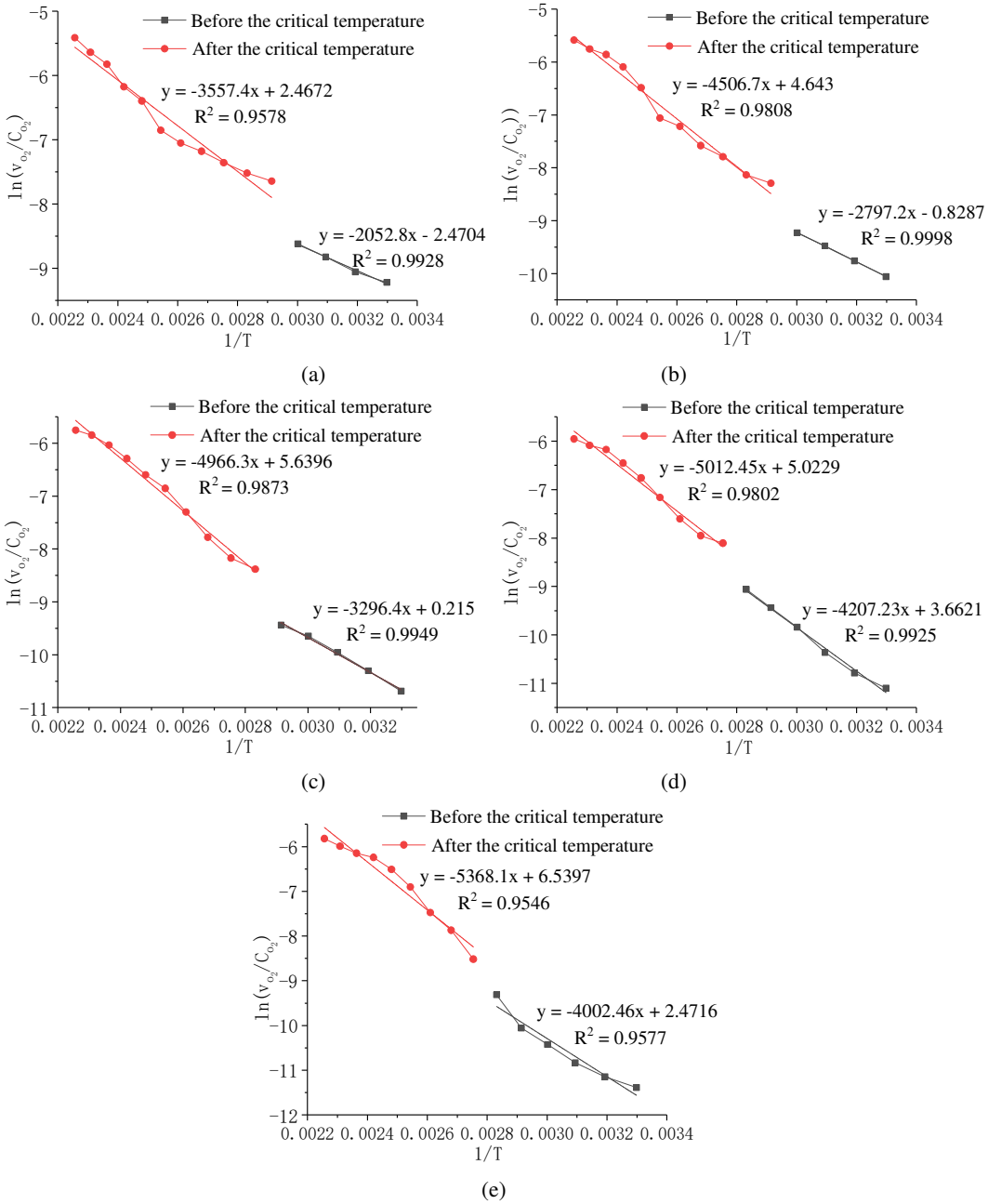

Fig. 6. $\ln(v_{o_2}^0/C_{o_2}^0)$ and 1/T relative curves of different particle sizes: (a) 0–0.9 mm, (b) 0.9–3 mm, (c) 3–5 mm, (d) 5–7 mm, (e) 7–10 mm.

CONCLUSIONS

(1) From analyzing the release law of the index gas, the law of CO gas release and the growth rate of oxygen consumption rate were basically consistent. The critical temperature of different coal samples was received as the basis for dividing the activation energy.

(2) After the division stage, the equation for the dynamic analysis fit better, and the equation can better reflect the relationship between $\ln(v_{o_2}^0/C_{o_2}^0)$ and $1/T$. Before the critical temperature, the apparent activation energy increased with the increase of the particle size. Since the particle size of 5–7 mm was the critical particle size, the apparent activation energy required for the particle size reaction was the most. After the critical temperature, as the particle size increased, the apparent activation energy also increased. The apparent activation energy differed greatly before and after the critical temperature. The apparent activation energy of the mixed particle size was small, as between 0–0.9 and 0.9–3 mm particle sizes.

(3) The apparent activation energy of the low-temperature oxidation reaction of 3^{-1} coal seam was less than that of the coal seam in 2^{-2mid}, indicating that the coal spontaneous combustion tendency of this coal seam was greater than that of the coal seam in 2^{-2mid}. Attention should be paid to the actual production process of the mine, to avoid harm to personnel and loss of property.

ACKNOWLEDGMENTS

Financial support for this study was kindly provided by National Natural Science Foundation Project of China (Nos. 5180-4246 and 5170-4226), and Doctor Start-up Project of Xi'an University of Science and Technology (No. 2017QDJ057), Xi'an, China.

REFERENCES

[1] G.B. Stracher, T.P. Taylor, Coal fires burning out of control around the world: thermodynamic recipe for environmental catastrophe, Int. J. Coal Geol. 59 (2004) 7–17.

[2] J.N. Carras, S.J. Day, A. Saghafi, D.J. Williams, Greenhouse gas emissions from low-temperature oxidation and spontaneous combustion at open-cut coal mines in Australia, Int. J. Coal Geol. 78 (2009) 161–168.

[3] S.T. Ide, F.M. Orr, Comparison of methods to estimate the rate of CO2 emissions and coal consumption from a coal fire near Durango, CO, Int. J. Coal Geol. 86 (2011) 95–107.

[4] A. Sarwar, M.N. Khan, K.F. Azhar, Kinetic studies of pyrolysis and combustion of Thar coal by thermogravimetry and chemometric data analysis, J. Therm. Anal. Calorim. 109 (2011) 97–103.

[5] J.A. MacPhee, J.P. Charland, L. Giroux, Application of TG–FTIR to the determination of organic oxygen and its speciation in the Argonne premium coal samples, Fuel Process Technol. 87 (2006) 335–341.

[6] L.I. Ali, A. Amin, A.M. Ibrahim, Thermal behavior and effect of compaction on phase changes and catalytic properties of some solid acid catalysts, Hung. J. Ind. Chem. 25 (1997) 1–6.

[7] A. Williams, M. Pourkashanian, J.M. Jones, The combustion of coal and some other solid fuels, Proc. Combust. Inst. 28 (2000) 2141–2162.

[8] M.E. Brown, M. Maciejewski, S. Vyazovkin, R. Nomen, J. Sempere, A. Burnham, et al., Computational aspects of kinetic analysis: part A: the ICTAC kinetics project-data, methods and results, Thermochim. Acta 355 (2000) 125–143.

[9] P. Budrugeac, The Kissinger law and the IKP method for evaluating the non-isothermal kinetic parameters, J. Therm. Anal. Calorim. 89 (2007) 143–151.

[10] D. Chen, D. Liu, H. Zhang, Y. Chen, Q. Li, Bamboo pyrolysis using TG–FTIR and a lab-scale reactor: analysis of pyrolysis behavior, product properties, and carbon and energy yields, Fuel 148 (2015) 79–86.

[11] R. Comesaña, J. Porteiro, E. Granada, J.A. Vilán, M.A. Álvarez Feijoo, P. Eguía, CFD analysis of the modification of the furnace of a TG–FTIR facility to improve the correspondence between the emission and detection of gaseous species, Appl. Energy 89 (2012) 262–272.

[12] J.L. Goldfarb, S. Ceylan, Second-generation sustainability: application of the distributed activation energy model to the pyrolysis of locally sourced biomass-coal blends for use in co-firing scenarios, Fuel 160 (2015) 297–308.

[13] Y.S. Nugroho, A.C. Mcintosh, B.M. Gibbs, Low-temperature oxidation of single and blended coals, Fuel 79 (2000) 1951–1961.

[14] B. Coda, L. Tognotti, The prediction of char combustion kinetics at high temperature, Exp. Therm. Fluid Sci. 21 (2000) 79–86.

[15] M. Duz, Y. Tonbul, A. Baysal, et al., Pyrolysis kinetics and chemical composition of Hazro coal according to the particle size, J. Therm. Anal. Calorim. 81 (2005) 395–398.

[16] D. Yu, M. Xu, J. Sui, et al. Effect of coal particle size on the proximate composition and combustion properties, Thermochim. Acta 439 (2005) 103–109.

[17] Y. Zhang, Y. Li, Y. Huang, et al., Characteristics of mass, heat and gaseous products during coal spontaneous combustion using TG/DSC–FTIR technology, J. Therm. Anal. Calorim. 131 (2018) 2963–2974.

[18] J. Deng, J.Y. Zhao, Y. Xiao, et al., Thermal analysis of the pyrolysis and oxidation behaviour of 1/3 coking coal, J. Therm. Anal. Calorim. 129 (2017) 1779–1786.

[19] C. Herce, B. de Caprariis, S. Stendardo, et al., Comparison of global models of sub-bituminous coal devolatilization by means of thermogravimetric analysis, J. Therm. Anal. Calorim. 117 (2014) 507–516.

[20] J. Wu, B. Wang, F. Cheng, Thermal and kinetic characteristics of combustion of coal sludge, J. Therm. Anal. Calorim. 129 (2017) 1899–1909.

[21] X. Cui, X. Li, Y. Li, et al., Evolution mechanism of oxygen functional groups during pyrolysis of Datong coal, J. Therm. Anal. Calorim. 129 (2017) 1169–1180.

[22] D. Wu, M. Schmidt, X. Huang, et al., Self-ignition and smoldering characteristics of coal dust accumulations in O_2/N_2 and O_2/CO_2 atmospheres, Proc. Combust. Inst. 36 (2017) 3195–202.

[23] Y. Xu, Y. Zhang, G. Zhang, et al., Pyrolysis characteristics and kinetics of two Chinese low-rank coals, J. Therm. Anal. Calorim. 122 (2015) 975–984.

[24] J. Gao, M. Chang, J. Shen, Comparison of bituminous coal apparent activation energy in different heating rates and oxygen concentrations based on thermogravimetric analysis, J. Therm. Anal. Calorim. 130 (2017) 1181–1189.

[25] K. Wang, J. Deng, Y. Zhang, et al., Kinetics and mechanisms of coal oxidation mass gain phenomenon by TG–FTIR and in situ IR analysis, J. Therm. Anal. Calorim. 132 (2018) 591–598.

[26] Z. Song, X. Huang, M. Luo, et al., Experimental study on the diffusion–kinetics interaction in heterogeneous reaction of coal, J. Therm. Anal. Calorim. 129 (2017) 1–13.